Spectral niches reveal taxonomic identity and complementarity in plant communities

Anna K. Schweiger[1,2,3]*, Jeannine Cavender-Bares[3], Philip A. Townsend[4], Sarah E. Hobbie[3], Michael D. Madritch[5], Shan Kothari[6], Jake J. Grossman[7], Hamed Gholizadeh[8], Ran Wang[9], John A. Gamon[9,10]

[1]Institut de recherche en biologie végétale, Université de Montréal, Montréal, Québec, Canada
[2]Département de sciences biologiques, Université de Montréal, Montréal, Québec, Canada
[3]Department of Ecology, Evolution and Behavior, University of Minnesota, Saint Paul, MN, USA
[4]Department of Forest and Wildlife Ecology, University of Wisconsin-Madison, Madison, WI, USA
[5]Department of Biology, Appalachian State University, Boone, NC, USA
[6]Department of Plant and Microbial Biology, University of Minnesota, Saint Paul, MN 55108, USA
[7]Arnold Arboretum of Harvard University, Boston, MA, USA
[8]Center for Applications of Remote Sensing, Department of Geography, Oklahoma State University, Stillwater, OK, USA
[9]Center for Advanced Land Management Information Technologies (CALMIT), School of Natural Resources, University of Nebraska-Lincoln, Lincoln, NE, USA
[10]Departments of Earth & Atmospheric Sciences and Biological Sciences, University of Alberta, Edmonton, Alberta, Canada

*Corresponding author, email: anna.k.schweiger@gmail.com, phone: +1 438 821 7554

Summary

- Plants' spectra provide integrative measures of their chemical, morphological, anatomical, and architectural traits. We posit that the degree to which plants differentiate in n-dimensional spectral space is a measure of niche differentiation and reveals functional complementarity.
- In both experimentally and naturally assembled communities, we quantified plant niches using hypervolumes delineated by either plant spectra or 10 functional traits. We compared the niche fraction unique to each species in spectral and trait spaces with increasing dimensionality, and investigated the association between the spectral space occupied, plant growth and community productivity.
- We show that spectral niches differentiated species better than their functional trait niches. The amount of spectral space occupied by individuals and plant communities increased with plant growth and community productivity, respectively. Further, community productivity was better explained by inter-individual spectral complementarity than by productive individuals occupying large spectral niches.
- The degree of differentiation in spectral space provides the conceptual basis for identifying plant taxa spectrally. Moreover, our results indicate that the size and position of plant spectral niches reflect ecological strategies that shape community composition and ecosystem function, with the potential to reveal insight in niche partitioning over large areas with spectroscopy.

Keywords

complementarity, functional traits, ecosystem function, Hutchinsonian niche, plant species identification, spectroscopy, spectral space, remote sensing

Introduction

The Hutchinsonian niche concept (Hutchinson, 1957) describes the niche as an n-dimensional hypervolume delineated by axes of environmental conditions (micro-habitat, abiotic factors, resources, predators etc.) within which populations of organisms can survive in the long term (Leibold, 1995; Bazzaz & Bazzaz, 1996; Silvertown, 2004). This understanding of niches combines two main lines of theory (Leibold, 1995; Chase & Leibold, 2003): the "habitat" niche, the conceptual space delineated by all environmental requirements of an organism (Grinnell, 1917), and the "functional" niche, the ecological role organisms play in their environment (Elton, 1927). These habitat- and function-centric concepts are connected, because organisms inevitably consume and supply resources when they occur in an environment supporting their needs. The realized niche thus entails both the requirements of a population of organisms in a particular environment (habitat factors) and their impact on that environment (biological interactions; Leibold, 1995; Chase & Leibold, 2003). However, quantifying plant niches in an n-dimensional environmental space that captures all biotic and abiotic factors important for determining the fitness of populations of organisms and their impacts on the environment and other trophic levels is challenging, especially outside of laboratory conditions (Bazzaz & Bazzaz, 1996; Violle & Jiang, 2009). The trait niche delineated by functional traits related to the performance of organisms and species along key environmental gradients (McGill *et al.*, 2006; Violle & Jiang, 2009) has been proposed as a means to overcome the problem of niche hyper-dimensionality. Niches of plants in trait space provide a mechanistic link to ecosystem function, since only certain combinations of traits appear to be successful (Reich *et al.*, 1997; Wright *et al.*, 2004) or are biologically possible. A key first step in defining the trait niche is prioritizing environmental factors that significantly influence plant fitness and determining which traits or trait syndromes best reflect the adaptations necessary for success in a particular environment (McGill *et al.*, 2006). But determining all environmental factors important for structuring plant communities and their relative importance is difficult, and there are practical and methodological limits to the (number of) traits or trait syndromes we can measure (Petchey & Gaston, 2006).

Plants partition resources in time and space as a result of contrasting ecological strategies, giving rise to biochemical, structural and phenological differences that affect optical properties of leaves and canopies. Spectral profiles of plants (the curves resulting from measuring plant spectra at high spectral resolution) are influenced by leaf traits (Gates *et al.*, 1965; Knipling,

1970; Jacquemoud & Baret, 1990; Ustin *et al.*, 2004; Cavender-Bares *et al.*, 2017), including pigment composition, micro- and macronutrient content, water content, specific leaf area (SLA), leaf surface and internal structure, and they are, when measured from a distance, also influenced by plant traits related to canopy architecture (Jacquemoud & Baret, 1990; Curran *et al.*, 2001; Slaton *et al.*, 2001; Sims & Gamon, 2002; Ollinger, 2011). Spectral profiles thus capture key differences in foliar chemistry, leaf anatomy, plant morphology, life history strategies, and responses to environmental variation, which have evolved over time and reflect ecological strategies (Ustin *et al.*, 2004; Cavender-Bares *et al.*, 2017) with consequences for ecosystem structure and function above- and belowground (Madritch *et al.*, 2014; Cavender-Bares *et al.*, 2017). The concept of spectral or optical types states that functionally distinct species (or other clades) occupy unique spectral spaces because of their specific chemical and structural characteristics (Palmer *et al.*, 2002; Rocchini *et al.*, 2010; Asner *et al.*, 2014; Féret & Asner, 2014), and there is evidence that spectral dissimilarity among species increases with functional dissimilarity (Asner & Martin, 2008; McManus *et al.*, 2016; Schweiger *et al.*, 2018) and evolutionary divergence time (Cavender-Bares *et al.*, 2016; McManus *et al.*, 2016; Schweiger *et al.*, 2018).

Here we combine the optical type concept with classical niche theory and present plant "spectral niches" - the spectral spaces occupied by plants - as an integrative approach to calculating niche size and its consequence for ecosystem function. We define the spectral niche as the n-dimensional hypervolume occupied by plants and delineated by spectral axes (which can be spectral bands, spectral indices, or other expressions of spectral variation) along which plants can vary. We quantify plant niches using hypervolumes estimated from convex hulls, which are the multivariate equivalents of range and independent of the shape of the distribution and correlation structure among measured variables (Cornwell *et al.*, 2006; Blonder *et al.*, 2014), and test three hypotheses associated with the degree of plant differentiation in spectral space: (H1) Plant species occupy distinct spectral niches as a consequence of contrasting functional attributes that are linked to resource acquisition; (H2) Plant individuals that occupy greater spectral niche space have higher performance in terms of growth due to increased intra-individual foliar variation in more complex canopies; (H3) More productive plant communities occupy greater spectral niche space, because of optical and functional complementarity.

We tested these hypotheses using data collected in a grassland and a forest biodiversity experiment – the Cedar Creek biodiversity (BioDIV) experiment (Tilman *et al.*, 1997) and the Forest and Biodiversity (FAB) experiment (Grossman *et al.*, 2017). We used leaf spectra and functional traits of 902 individuals from 14 grassland–savanna perennials sampled in 35 plots in BioDIV and aboveground biomass determined in the same plots in July 2015 (H1, H3); and leaf spectra, plant height and diameter measurements of 537 individuals from 12 tree species sampled in 68 plots in FAB in July 2016 (H2, H3). In addition, we were interested in the stability of species' spectral niches in space, time and across measurement scales. We thus tested the degree to which species identification models developed in BioDIV correctly differentiate species measured in naturally assembled grassland communities, and at a different time and measurement scale using three additional datasets: Leaf spectra and functional traits of 281 individuals from seven grassland–savanna perennials collected in July 2016 in 19 plots of an old fields chronosequence taken out of agricultural use between 1928 and 2015 (Inouye *et al.*, 1987; Clark *et al.*, 2019); leaf spectra and functional traits of 243 individuals from nine species collected in 14 plots in BioDIV in August 2015; and remotely sensed spectra collected with an imaging spectrometer mounted on a robotic cart (Wang *et al.*, 2016) in 18 plots of the BioDIV experiment in July 2015.

Material and Methods

Spectral data

We measured leaf spectra using a leaf-clip assembly and two portable field spectrometers (SVC HR-1024i, Spectra Vista Corp., Poughkeepsie, NY; and PSR +, Spectral Evolution Inc., Lawrence, MA) covering the wavelength range from 350 nm to 2500 nm in 1024 spectral bands. We used the SVC instrument for measuring grassland-savanna perennials and the PSR+ for measuring tree species. To characterize one individual spectrally, we measured the reflectance of either three or five mature, healthy leaves per individual depending on plant height. Spectra were automatically calibrated for dark current and stray light, and referenced to the white calibration disc of the leaf clip approximately every 10 minutes. Spectral data processing included correcting discontinuities at the sensor overlap regions between the Si and first InGaAs sensor (around 1000 nm) and between the first and second InGaAs sensor (around 1900 nm), removing

noisy regions at the beginning and end of the spectrum, and interpolating spectra to 1 nm resolution. In addition, we collected leaf level spectral with an imaging spectrometer (E Series, Headwall Photonics, Fitchburg, MA) mounted on an automated tram (also referred to as spectral images; see Gamon *et al.*, 2006 for details). Each processed image consisted of 1,000 x 1,000 pixels with 1 mm spatial resolution covering the visible and near-infrared regions (400–990 nm) in 924 spectral bands. Again, spectra were resampled to 1 nm spectral resolution and noisy regions at the beginning and end of the spectrum were excluded. For spectral processing we used the spectrolab (Meireles *et al.*, 2017) package in R (R Core Team, 2019). The BioDIV July dataset consisted of 902 individuals (ind.) from 14 species: *Achillea millefolium* L. (49 ind.), *Amorpha canescens* Pursh (28 ind.), *Andropogon gerardii* Vitman (162 ind.), *Asclepias tuberosa* L. (70 ind.), *Lespedeza capitata* Michx. (99 ind.), *Liatris aspera* Michx. (49 ind.), *Lupinus perennis* L. (121 ind.), *Panicum virgatum* L. (49 ind.), *Petalostemum candidum* (Willd.) Michx. (28 ind.), *Petalostemum purpureum* (Vent.) Rydb. (52 ind.), *Petalostemum villosum* Nutt. (42 ind.), S*chizachyrium scoparium* (Michx.) Nash (76 ind.), *Solidago rigida* L. (50 ind.), *Sorghastrum nutans* (L.) Nash (27 ind.). The old fields dataset consisted of 281 individuals from seven species: *Agropyron repens* (L.) P. Beauv. (48 ind.), *Berteroa incana* (L.) DC. (29 ind.), *Lespedeza capitata* Michx. (29 ind.), *Panicum virgatum* L. (27 ind.), *Poa pratensis* L. (67 ind.), *Rumex acetosella* L. (27 ind.), *Schizachyrium scoparium* (Michx.) Nash (54 ind.). The BioDiv August dataset consisted of 243 individuals from nine species: *Achillea millefolium* L. (20 ind.), *Amorpha canescens* Pursh (18 ind.), *Andropogon gerardii* Vitman (27 ind.), *Lespedeza capitata* Michx. (30 ind.), Liatris aspera Michx. (18 ind.), *Petalostemum purpureum* (Vent.) Rydb. (33 ind.), *Schizachyrium scoparium* (Michx.) Nash (41 ind.), *Solidago rigida* L. (32 ind.), *Sorghastrum nutans* (L.) Nash (24 ind.). The spectral image data consisted of 2237 pixels from seven species: *Achillea millefolium* L. (264 pixels), *Andropogon gerardii* Vitman (283 ind.), *Asclepias tuberosa* L. (422 pixels), *Lespedeza capitata* Michx. (149 pixels), *Monarda fistulosa* L. (242 pixels), *Panicum virgatum* L. (388 pixels), *Schizachyrium scoparium* (Michx.) Nash (241 pixels), *Solidago rigida* L. (248 pixels). And the FAB dataset consisted of 537 individuals from 12 species: *Acer negundo* L. (30 ind.), *Acer rubrum* L. (47 ind.), *Betula papyrifera* Marshall (44 ind.), *Juniperus virginiana* L. (39 ind.), *Pinus banksiana* Lamb. (47 ind.), *Pinus resinosa* Aiton (52 ind.), *Pinus strobus* L. (47 ind.), *Quercus alba* L. (42 ind.), *Quercus*

ellipsoidalis E.J.Hill (49 ind.), *Quercus macrocarp*a Michx. (50 ind.), *Quercus rubra* L. (39 ind.), *Tilia americana* L. (51 ind.).

Functional traits

We determined the following functional traits for all individuals of grassland–savanna perennials measured spectrally with the leaf clip: foliar nitrogen, carbon, non-structural carbohydrate, hemicellulose, cellulose, and lignin concentration (%), and the content of chlorophyll a and b, beta-carotene, lutein, violaxanthin, antheraxanthin, and zeaxanthin pigments (μmol m^{-2}). Foliar traits were predicted using partial least squares regression (PLSR) models (Wold *et al.*, 1983) developed from chemical assays of leaf tissue samples and corresponding level spectra. Leaf tissue samples were collected in the summers of 2015 and 2016 at the CCESR and encompassed 62 species; all chemical trait analyses were performed at the University of Minnesota following methods described in (Schweiger *et al.*, 2018). We summarized chlorophyll content as chlorophyll a plus chlorophyll b; and we expressed beta-carotene and lutein content, and the size of the xanthophyll pigment pool (VAZ = violaxanthin plus antheraxanthin plus zeaxanthin) as ratios relative to chlorophyll content to indicate contrasting photosynthetic behavior and photoprotective capacity among plants (Gamon *et al.*, 1997; Gamon & Berry, 2012). We tested for differences among species functional traits using Tukey's honest significant difference (HSD) post hoc tests and the R package agricolae (de Mendiburu, 2017). Further, since we expected species separability to increase with phylogenetic distance (Schweiger *et al.*, 2018), we tested for phylogenetic signal of each trait using Blomberg's K statistic (Blomberg *et al.*, 2003) as implemented in the R package picante (Kembel *et al.*, 2010) and the phylogeny reconstructed by (Kothari *et al.*, 2018) with one missing species (*Petalostemum candidum* (Willd.) Michx.) added manually with phytools (Revell, 2012; for details, see also Table S5). For all trees in our study we used individual tree height (cm) and basal diameter (cm) as measures of growth (Grossman *et al.*, 2017).

Species spectral and functional niches

We calculated the niche fraction unique to each of the 14 species sampled in BioDIV in spectral space and functional trait space of increasing dimensionality using the R package hypervolume

(Blonder *et al.*, 2014). We randomly selected between 2 and 21 spectral bands and between 2 and 10 functional traits as axes delineating species' spectral and functional niches, respectively, and repeated each selection 50 times; functional traits were z-standardized. We projected all individuals into the resulting spectral and functional trait spaces, and calculated the fraction of the hypervolume unique to each species (i.e. the hypervolume that is occupied by the focal species and not overlapped by any other species).

Since it is difficult to show more than three or four niche dimensions in one graph, we used linear discriminant analysis (LDA) to illustrate species spectral and functional dissimilarity in niche spaces delineated by the main axes of spectral and functional variation. In our case, linear discriminants (LDs) are linear combinations of all band-wise reflectance and functional trait values, respectively, which re-project observations into a new coordinate system while maximizing the differences between groups; our grouping variable was species identity. For LDA we used the R package MASS (Venables & Ripley, 2002); for interactive 3D graphics illustrating species niche shifts with changes in community diversity we used plotly (Sievert *et al.*, 2017).

Species identification models

We tested the degree to which plant species can be correctly identified based on spectra and functional traits with partial least squares discriminant analysis (PLSDA) as implemented in the R packages pls (Mevik *et al.*, 2018) and caret (Kuhn, 2018). We chose the number of samples for model training depending on sample size: For the BioDIV model based on data sampled in July and for the old fields chronosequence model we used random draws of 20 individuals per species for model training; for the BioDIV model based on data sampled in August we used random draws of 10 individuals per species; and for the imaging spectroscopy model we used random draws of 50 pixels per species. The remaining data were used for validation and for evaluating model fit; all statistics and graphs are based on the validation results. For each dataset, we performed 100 PLSDA model iterations always using new random draws of training samples and selected the optimal number of components based on the minimum of the root mean squared error of prediction (RMSEP) for the test samples. We tested for significant differences in RMSEP values using Tukey's HSD test as implemented in the R package agricolae (de Mendiburu, 2017), and used the smaller number of components when models performed

similarly ($p > 0.05$). We investigated which wavelengths and functional traits contributed most to species separability using PLSDA loadings. For the species identification models based on spectral images, we extracted sunlit pixels from seven clearly identifiable species using ENVI 5.4 (Exelis Visual Information Solutions, Boulder, CO). To investigate model transferability, we subset each dataset to match the species sampled in both datasets. For each of the subsets, we calibrated new PLSDA models as described above, always using 20 randomly selected samples per species for training, and the remaining data for testing and model evaluation. We assessed model transferability i) in space by applying the BioDIV July model to the old fields chronosequence data and vice versa, ii) in time by applying the BioDIV July model to the BioDIV August data and vice versa, and iii) across sampling scales by applying the BioDIV July model to spectral image data.

Spectral space occupied by individuals and plant communities

We tested the degree to which the spectral space occupied by individual plants predicts plant growth by fitting regression models between the spectral space occupied by trees sampled in FAB and two measures of growth, tree height (cm) and basal diameter (cm). We assessed model performance based on the coefficient of determination (R^2) and the RMSEP. Next, we tested the degree to which the spectral space occupied by plant communities predicts aboveground productivity. In BioDIV we used biomass (g m^{-2}, dry weight) determined in clipstrips as a measure of aboveground net primary productivity. In FAB we used overyielding as a measure of the net biodiversity effect (NBE), which we partitioned into complementary (CE) and selection effects (SE), following (Loreau & Hector, 2001). Biomass for NBE, SE and CE calculations was determined from allometrically derived incremental stem biomass (kg y^{-1}; see Grossman *et al.*, 2017 for details). We did not calculate and partition the NBE in BioDIV because monocultures are not replicated in this experiment. Niche size, as other measures of the spread of variables, is known to be positively correlated with sample size (Cornwell *et al.*, 2006). We thus used the same number of randomly selected individuals per community to calculate the occupied spectral space. For the BioDIV data collected with the leaf clip, we used spectra of 12 randomly selected individuals per plot resulting in a total of 30 communities used for analysis. For the BioDIV data collected with the imaging spectrometer, we randomly extracted 30 pixels per plot; spectra were corrected for soil effects following (Gholizadeh *et al.*, 2018). For FAB, we used spectra of nine

randomly selected individuals per plot, resulting in a total of 68 communities used for analysis. We reduced data dimensionality to the first three principal component (PC) axes, which explained more than 98% of the total spectral variation in the leaf clip data (BioDIV and FAB) and more than 96% of the total spectral variation in the proximal remote sensing data, respectively, and calculated the spectral space occupied per community using the hypervolume package (Blonder *et al.*, 2014) in R. We tested the association between the spectral space occupied by plant communities and community productivity using linear regression models, and assessed model performances based on the R^2 and RMSEP. In addition, we tested the degree to which the spectral space occupied by plant communities increases with species richness.

Data availability

The data used in this manuscript are publicly available through EcoSIS https://ecosis.org (spectral data), the Cedar Creek Ecosystem Science Reserve http://www.cedarcreek.umn.edu/research/data (biomass data), and LPDAAC https://lpdaac.usgs.gov/dataset_discovery/community/community_products_table/hwhypccmn1mm_v001 (spectral images, DOI: 10.5067/Community/Headwall/HWHYPCCMN1MM.001).

Results

Species spectral niches were more distinct than their trait-based niches calculated from the 10 chemical and structural foliar traits (carbon, nitrogen and carbon fraction concentration and the contents of chlorophyll and carotenoid pigments; see Methods) measured in our study. The fraction of the niche space unique to each of the 14 species of grassland–savanna perennials increased with the dimensionality of spectral and functional trait space (Fig. 1). However, while each focal species occupied a hypervolume that was at least 90% unique to the species after including 15 randomly selected spectral bands as axes (Fig. 1a, Table S1), not all focal species reached the same level of uniqueness in functional trait space after including all 10 functional traits as axes (Fig. 1b, Table S2). Greater distinctiveness of species spectral niches as compared to their functional niches was confirmed when projecting species' positions into spectral and functional spaces reduced to their main axes of variation. In spectral space, all non-graminoids species clearly separated along the first four linear discriminate axes (LDs, Fig. 2a-b), and LDs

11 and 12 separated the graminoids (Fig. 2c). In functional trait space, however, only a few species formed distinct clusters, and we found no combination of LDs that separated the four graminoids from each other (Fig. 2d-f). The likely reason being the substantial degree of intraspecific variation across all measured traits (Fig. S1) and the lack of a particular trait or traits that differed significantly among all species (Fig. S2, Table S3). This is also illustrated by the high degree of overlap among species niches in two-dimensional trait space (Fig. S3b); although legumes and graminoids clustered somewhat separately from other species along carbon content, and nitrogen content and carbon fraction axes, respectively. Species' niche overlap was also pronounced in two-dimensional spectral space delineated by the 10 most variable spectral bands, but spectrally distinct species already started emerging (Fig. S3a).

Species identification models based on spectra (65% - 98% accuracy per species, Figs 3a, S4a, Table S4) consistently outperformed species identification models based on functional traits (47% - 97% accuracy per species, Figs 3b, S4b, Table S4), probably due to the smaller overlap (Fig. 1) and greater distance (Fig. 2) between species' niches in spectral space compared to trait space. The spectral bands contributing most to species' separability aligned with absorption features related to leaf chlorophyll, carotenoid, lignin and protein content (Fig S5a). These foliar traits also contributed most to species separability in functional trait space (Fig. S5b) and all of them, except for chlorophyll content, showed evidence of phylogenetic signal (Table S5, Fig. S6). The better performance of species identification models based on spectra compared to models based on functional traits was confirmed in the old fields chronosequence (93% compared to 69% overall accuracy) and in the BioDIV experiment sampled later in the season (96% compared to 74% overall accuracy), and species were also to 93% correctly identified from the spectral images (Figs S7-S9, Table S4). Generally, spectral models were more transferable across sites and functional trait models were more transferable in time (Table S6). However, it was not possible to successfully transfer a species identification model calibrated using leaf-clip data to the spectral images collected at the same time, likely because the sampling method normalized for illumination and removed effects of plant architecture and atmosphere, which are important sources of spectral variation at the canopy level.

The spectral space occupied by individual trees - a measure of intra-individual spectral variation - was linked to the total variation in the tree height and diameter (Fig. 4), likely because trees that grow more tend to have larger, more complex canopies and higher foliar plasticity than

trees that grow less. Over time, taller trees seem to be able to sustain and perhaps even increase the benefits gained from harnessing a more diverse light environment (Figs 4b, 4d), pointing towards size-asymmetric (size-dependent) light competition (Schwinning & Weiner, 1998) among the young trees in FAB. The spectral space occupied by individuals was more closely associated with tree diameter than tree height. One likely explanation being that once trees are taller than their neighbors, it may be more advantageous to invest in mechanical stability and horizontal canopy extension than in vertical growth to maximize light interception.

The spectral space occupied by plant communities in BioDIV explained 44% of the total variation in aboveground productivity when estimated from spectra measured with the leaf clip (Fig. 5a) and 31% when estimated from the spectral images (Fig. 5b). Likewise, the spectral space occupied increased with the number of species per plant community (Fig. 5c). Thus, the size of the spectral niche occupied by plant communities provides an alternative measure of spectral diversity that is similarly predictive of productivity as other measures of biodiversity reported in this experiment (see Schweiger *et al.*, 2018 and references therein). In FAB, we used overyielding (i.e. the access biomass produced by mixed species plots compared to what would be expected based on their monoculture yields) as a measure of the net biodiversity effect (NBE); and we partitioned the NBE into its two components, complementary (the positive effects of diverse resource use strategies and positive interactions among plants on productivity) and selection effects (the influence of plants with particular traits on productivity, following Loreau & Hector, 2001). The spectral space occupied by tree communities in FAB explained 42% of overyielding (Fig. 6a) and increased with the number of species per community (Fig. 6b). Partitioning the NBE, into its two components revealed a positive relationship between the spectral space occupied by communities and complementarity (Fig. 6c), while the association with the selection effect was negative (Fig. 6d). In other words, compared to less productive communities more productive communities did on average not harbor more highly productive individuals which occupy larger spectral spaces, but rather more spectrally dissimilar and complementary species that collectively contributed to the large spectral space occupied by these communities.

Discussion

Plants display themselves towards the sky with contrasting optical patterns linked to biochemical, anatomical and morphological plant traits that have evolved over time and influence their spectral response (Ustin & Gamon, 2010; Cavender-Bares *et al.*, 2017). Not all functional traits of plants, including hydraulic and root traits, and traits specific to organs that interact minimally with light, including seeds, can be spectrally detected. However, plant spectra integrate many aspects of plant form and function offering an effective and novel way to quantify plant niches in n-dimensional space (*sensu* Hutchinson, 1957). Here we show that spectral differentiation – the degree to which species and individuals occupy distinct spectral spaces – is an important and useful measure of complementarity and provides a practical means of identifying plant species or other clades or functional groups with spectra.

Spectra of plants captured more of the total variation in plant characteristics than the set of functional traits measured in our study. Projecting species into functional and spectral spaces with increasing dimensionality gradually reduced the overlap among species (Fig. 1). However, species functional niches contracted to a lesser degree than their spectral niches, leading to spectral species identification models consistently outperforming species identification models based on functional traits (Table S4). To some extent, this effect could be due to redundancy in our metrics of function. Plant functional traits reflect their phylogenetic legacies as well as environmental adaptations. In our case, light gradients are probably the dominating source of environmental variation, and all leaf traits measured in our study are to some degree influenced by variation in light. For instance, the degree of correlation between chlorophyll and carotenoid pigment levels reflects biochemical adaptation to different light environments; with tight correlations indicating their common role in light harvesting and weak correlations indicating a stress response (Gamon & Berry, 2012). Likewise, the contents of different carbon fractions are tied to morphological adaptations (such as leaf thickness and SLA) to light gradients within canopies (Niinemets, 2007). In this way, what we think of as multiple traits can also be thought of as different proxies for the same or overlapping traits.

Misclassifications occurred more often among closely related than among distantly related species (Figs 3, S4a, S7a, S8a), likely due to the similarity in functional traits (Tables S3, S5, Fig. S6) and spectra among close relatives (Cavender-Bares *et al.*, 2016; Schweiger *et al.*, 2018). The spectral regions that contributed most to species separability aligned with absorption

features for proteins and lignin content (Fig. S5a; see e.g. Curran, 1989), functional traits associated with the trade-off between fast and slow return on investment (Reich *et al.*, 1997; Wright *et al.*, 2004) suggesting the relevance of different resource use strategies for structuring plant communities and community productivity (Reich *et al.*, 1997). In addition, chlorophyll content and xanthophyll cycle pigment pool size contributed substantially to species separability, highlighting that prairie ecosystems harbor species with different strategies for light capture and photoprotection (Kothari *et al.*, 2018). These sets of traits also relate to canopy structure (e.g. leaf display) and so can tie to higher level spectral and plant traits at the canopy scale.

The images collected by the mobile tram capture the spectra of leaves in their natural orientation and illumination, as would be seen in remote sensing. The high classification accuracy of spectral species identification models based on spectral images is a promising result for high resolution remote sensing approaches to species identification (e.g. using unmanned aerial vehicles, UAV's). For instance, imaging spectroscopy that can resolve canopies, i.e. with pixel sizes smaller than the typical species crown (Arroyo-Mora *et al.*, 2019), has tremendous potential for detecting biodiversity and quantifying spectral niches, given that a training dataset of plants or plant leaves can be identified directly from the images, or on the ground and geo-referenced.

Spectral models were more transferable in space, while functional trait models were more transferable in time (Table S6), pointing towards differences in the relative importance of biochemical vs. morphological/anatomical trait variation for species differentiation. Chemical characteristics of leaves change as leaves age and spectra capture these phenological differences more completely than a set of foliar traits (Chavana-Bryant *et al.*, 2017), making it easier to transfer species identification models based on a limited number of foliar traits in time compared to species identification models based on spectra. Leaf morphology and anatomy, including surface structure and leaf thickness, are often less variable within species than leaf chemistry (Valladares *et al.*, 2000). Morphological and anatomical leaf traits were not included in the set of functional traits we measured, but they are captured by spectral measurements (Cavender-Bares *et al.*, 2017), likely making it easier to transfer species identification models based on spectra in space. However, it is worth noting that our study sites were spatially close and similar in their environmental characteristics, including soil, and we expect decreasing spatial transferability of spectral models with increasing environmental dissimilarity among sites.

411 The positive relationship between the intra-individual spectra variation and tree height
412 and diameter (Fig. 4) supports our hypothesis that plants occupying more spectral space have
413 greater performance in terms growth. Light is likely the most variable resource for the young
414 trees in the FAB experiment, leading to adaptations in leaf traits, including SLA, pigment and
415 nitrogen content (Valladares *et al.*, 2000; Rozendaal *et al.*, 2006), which all influence the spectral
416 response. The foliar plasticity in response to diverse light environments might create a self-
417 reinforcing system leading to increased plant growth, which, in turn, modifies and likely
418 increases intra-individual spectral variation through increased leaf area index (LAI) generating
419 even more pronounced light gradients, as found in other tree diversity experiments (Williams *et*
420 *al.*, 2017). Notably, while tree growth in FAB was positively correlated with intra-individual
421 spectral variation (Fig. 4), the size of the spectral space occupied by productive individuals did
422 not explain well the association between productivity and the spectral space occupied by
423 communities (Fig. 6a). In our case, it appears that the spectral space occupied by productive
424 plant communities is dominated by spectral complementarity, which has been identified as an
425 important factor for light resource partitioning among evergreen and deciduous trees (Gamon *et*
426 *al.*, 2016; Springer *et al.*, 2017). Again, the size of the spectral space occupied by spectrally
427 diverse communities can be explained by a positive feedback, where spectral dissimilarity results
428 in and is a consequence of greater resource use and increased growth. The spectral space
429 occupied by plant communities can thus be interpreted as a measure of functional complexity,
430 because more spectrally dissimilar species tend to be more functionally dissimilar (Asner &
431 Martin, 2008; Schweiger *et al.*, 2018).
432 Investigating changes in species spectral niche size, overlap and position in relation to
433 changes in environmental conditions presents an interesting avenue for the future studies. Niches
434 of species can be distinct from each other due to niche separation, niche differentiation or by
435 chance, due to stochastic factors influencing the occurrence of a particular set of individuals with
436 distinct traits in one particular place and time (Cornwell *et al.*, 2006). Investigating species
437 trajectories and niche sizes in spectral space and identifying the absorption features that
438 contribute most to niche shifts and that separate species best under certain environmental
439 conditions can indicate temporal and spatial resource partitioning (Pickett & Bazzaz, 1978).
440 Empty volumes in the spectral space occupied by plant communities might indicate colonization
441 or invasion potential, or, alternatively, biologically unrealized spectral types. In our case, species

niche sizes and positions in trait space changed depending on the diversity level of the plant community (Fig. S10), which was in line with species-specific trait changes with community diversity (Fig. S12, Tables S7, S8, Notes S1). Species' niche sizes in spectral space changed depending on community diversity as well, but their positions remained more stable (Fig. S11), providing an additional explanation for the high classification accuracies of spectral species identification models (Table S4). Also, it is likely that biophysical trade-offs in plant functional traits, such as between nitrogen content or photosynthetic capacity and SLA (see e.g. Reich *et al.*, 1997; Wright *et al.*, 2004) impose boundaries on spectral profiles limiting the degree of spectral variation possible. This might result both in species spectra diverging or converging in particular cases, and in species, lineages or functional groups following unique trajectories in spectral space depending on environmental conditions and phenology. Incorporating spectral niche shift of plants in identification models could allow groups of plants that are spectrally similar at one point in time to be differentiated with time series of spectral data, which would be particularly useful in diverse environments and for large-scale studies.

The concept of the niche integrates many biological characteristics of organisms, providing a conceptual synthesis for the functioning of ecosystems (Leibold, 1995). The integrative nature of plant spectra and their links to plant form, function and phylogeny (Ustin & Gamon, 2010; Cavender-Bares *et al.*, 2017; Schweiger *et al.*, 2018) make the spectral niche concept particularly relevant to ecology. Plants with contrasting functional attributes occupy distinct spectral spaces allowing plant species, lineages and functional groups to be identified spectrally. Furthermore, evaluation of the occupied hypervolumes and the position of individuals, taxonomic groups and communities in spectral space with leaf-level and imaging spectroscopy provides a novel way of assessing plant-plant and plant-resource interactions. The spectral niche concept unites ecological theory and biology with the physics of light capture and distribution to reveal mechanisms of plant species coexistence, their distribution, abundance and diversity.

Acknowledgements

We thank Brett Fredericksen for leaf level sampling and HPLC, Ian Carriere, Erin Murdock, Lewis French and Travis Cobb for leaf level sampling, Cathleen Lapadat for chemical assays and HPLC, and Brian Leavitt for curating the tram data. Thanks to Etienne Laliberté for comments on the manuscript. Funding was provided by the National Science Foundation and National Aeronautics and Space Administration through the Dimensions of Biodiversity program (DEB-1342872 grant to JCB and SEH, DEB-1342778 grant to PAT, DEB-1342827 grant to MDM, DEB-1342823 grant to JAG); by the Cedar Creek National Science Foundation Long-Term Ecological Research program (DEB-1234162); iCORE/AITF (G224150012 and 200700172), NSERC (RGPIN-2015-05129), and CFI (26793) grants to JAG; by the University of Minnesota's Doctoral Dissertation Fellowship and the University of Minnesota Department of Ecology, Evolution, and Behavior's Summer Research, and Crosby, Rothman, Wilkie, Anderson, and Dayton funds to JJG.

Author contributions

The ideas presented in this article originated through many discussions during the Dimensions of Biodiversity project "Linking remotely sensed optical diversity to genetic, phylogenetic and functional diversity to predict ecosystem processes" conceptualized by JCB, PAT, SEH, MDM and JAG. AKS, JCB, PAT and JAG planned data collection in BioDIV. JCB, JJG, SK and SEH planned data collection in FAB. JAG and RW designed the spectral tram system. AKS, RW, and JAG collected data in BioDIV. JJG and SK collected data in FAB and calculated measures of tree growth. AKS analyzed the data and wrote the first draft of the manuscript, with input from JCB and JAG. All authors contributed substantially to revisions.

References

Arroyo-Mora JP, Kalacska M, Inamdar D, Soffer R, Lucanus O, Gorman J, Naprstek T, Schaaf ES, Ifimov G, Elmer K. 2019. Implementation of a UAV–Hyperspectral Pushbroom Imager for Ecological Monitoring. *Drones* 3(1): 12.

Asner GP, Martin RE. 2008. Airborne spectranomics: mapping canopy chemical and taxonomic diversity in tropical forests. *Frontiers in Ecology and the Environment* **7**(5): 269-276.

Asner GP, Martin RE, Carranza-Jiménez L, Sinca F, Tupayachi R, Anderson CB, Martinez P. 2014. Functional and biological diversity of foliar spectra in tree canopies throughout the Andes to Amazon region. *New Phytologist* **204**(1): 127-139.

Bazzaz FA, Bazzaz F. 1996. Plants in changing environments: linking physiological, population, and community ecology: Cambridge University Press.

Blomberg SP, Garland Jr T, Ives AR. 2003. Testing for phylogenetic signal in comparative data: behavioral traits are more labile. *evolution* **57**(4): 717-745.

Blonder B, Lamanna C, Violle C, Enquist BJ. 2014. The n-dimensional hypervolume. *Global Ecology and Biogeography* 23(5): 595-609.

Cavender-Bares J, Gamon JA, Hobbie SE, Madritch MD, Meireles JE, Schweiger AK, Townsend PA. 2017. Harnessing plant spectra to integrate the biodiversity sciences across biological and spatial scales. *American journal of botany* **104**(7): 966-969.

Cavender-Bares J, Meireles JE, Couture JJ, Kaproth MA, Kingdon CC, Singh A, Serbin SP, Center A, Zuniga E, Pilz G. 2016. Associations of leaf spectra with genetic and phylogenetic variation in Oaks: Prospects for remote detection of biodiversity. *Remote Sensing* **8**(3): 221.

Chase JM, Leibold MA. 2003. Ecological niches: Linking classical and contemporary approaches. Chicago; London: University of Chicago Press.

Chavana-Bryant C, Malhi Y, Wu J, Asner GP, Anastasiou A, Enquist BJ, Caravasi EGC, Doughty CE, Saleska SR, Martin RE. 2017. Leaf aging of Amazonian canopy trees as revealed by spectral and physiochemical measurements. *New Phytologist* 214(3): 1049-1063.

Clark AT, Knops JM, Tilman D. 2019. Contingent factors explain average divergence in functional composition over 88 years of old field succession. *Journal of Ecology* **107**(2): 545-558.

Cornwell WK, Schwilk DW, Ackerly DD. 2006. A trait-based test for habitat filtering: convex hull volume. *Ecology* **87**(6): 1465-1471.

Curran PJ. 1989. Remote sensing of foliar chemistry. *Remote Sensing of Environment* **30**(3): 271-278.

Curran PJ, Dungan JL, Peterson DL. 2001. Estimating the foliar biochemical concentration of leaves with reflectance spectrometry: testing the Kokaly and Clark methodologies. *Remote Sensing of Environment* **76**(3): 349-359.

de Mendiburu F. 2017. agricolae: Statistical Procedures for Agricultural Research, R package version 1.2-8. *https://CRAN.R-project.org/package=agricolae*.

Elton CS. 1927. *Animal ecology*. London: Sidgwick & Jackson.

Féret J-B, Asner GP. 2014. Mapping tropical forest canopy diversity using high-fidelity imaging spectroscopy. *Ecological Applications* **24**(6): 1289-1296.

Gamon J, Serrano L, Surfus J. 1997. The photochemical reflectance index: an optical indicator of photosynthetic radiation use efficiency across species, functional types, and nutrient levels. *Oecologia* **112**(4): 492-501.

Gamon JA, Berry JA. 2012. Facultative and constitutive pigment effects on the Photochemical Reflectance Index (PRI) in sun and shade conifer needles. *Israel Journal of Plant Sciences* **60**(1-2): 85-95.

Gamon JA, Cheng Y, Claudio H, MacKinney L, Sims DA. 2006. A mobile tram system for systematic sampling of ecosystem optical properties. *Remote Sensing of Environment* **103**(3): 246-254.

Gamon JA, Huemmrich KF, Wong CY, Ensminger I, Garrity S, Hollinger DY, Noormets A, Peñuelas J. 2016. A remotely sensed pigment index reveals photosynthetic phenology in evergreen conifers. *Proceedings of the National Academy of Sciences* 113(46): 13087-13092.

Gates DM, Keegan HJ, Schleter JC, Weidner VR. 1965. Spectral properties of plants. *Applied Optics* 4(1): 11-20.

Gholizadeh H, Gamon JA, Zygielbaum AI, Wang R, Schweiger AK, Cavender-Bares J. 2018. Remote sensing of biodiversity: Soil correction and data dimension reduction methods improve assessment of α-diversity (species richness) in prairie ecosystems. *Remote Sensing of Environment* **206**: 240-253.

Grinnell J. 1917. The Niche-Relationships of the California Thrasher. *The Auk* **34**(4): 427-433.

554 **Grossman JJ, Cavender-Bares J, Hobbie SE, Reich PB, Montgomery RA. 2017.** Species
555 richness and traits predict overyielding in stem growth in an early-successional tree diversity
556 experiment. *Ecology* **98**(10): 2601-2614.
557 **Hutchinson GE. 1957.** Concluding remarks. Cold Spring Harbor Symposium on Quantitative
558 Biology **22**: 415-427.
559 **Inouye RS, Huntly NJ, Tilman D, Tester JR, Stillwell M, Zinnel KC. 1987.** Old-field
560 succession on a Minnesota sand plain. *Ecology* 68(1): 12-26.
561 **Jacquemoud S, Baret F. 1990.** PROSPECT: A model of leaf optical properties spectra. *Remote*
562 *Sensing of Environment* **34**(2): 75-91.
563 **Kembel SW, Ackerly DD, Blomberg S, Cornwell W, Cowan P, Helmus M, Morlon H,**
564 **Webb C. 2010**. R tools for integrating phylogenies and ecology. *R Package 'picante*.
565 **Knipling EB. 1970.** Physical and physiological basis for the reflectance of visible and near-
566 infrared radiation from vegetation. *Remote Sensing of Environment* **1**(3): 155-159.
567 **Kothari S, Cavender-Bares J, Bitan K, Verhoeven AS, Wang R, Montgomery RA, Gamon**
568 **JA. 2018.** Community-wide consequences of variation in photoprotective physiology among
569 prairie plants. *Photosynthetica*.
570 **Kuhn M. Contributions from Wing J, Weston S, Williams A, Keefer C, Engelhardt A,**
571 **Cooper T, Mayer Z, Kenkel B, the R Core Team, Benesty M, Lescarbeau R, Ziem A,**
572 **Scrucca L, Tang Y, Candan C and Hunt T 2018.** caret: Classification and Regression
573 Training. R package version 6.0-81. https://CRAN.R-project.org/package=caret.
574 **Leibold MA. 1995.** The Niche Concept Revisited: Mechanistic Models and Community
575 Context. *Ecology* **76**(5): 1371-1382.
576 **Loreau M, Hector A. 2001.** Partitioning selection and complementarity in biodiversity
577 experiments. *Nature* **412**(6842): 72-76.
578 **Madritch MD, Kingdon CC, Singh A, Mock KE, Lindroth RL, Townsend PA. 2014.**
579 Imaging spectroscopy links aspen genotype with below-ground processes at landscape scales.
580 *Philosophical Transactions of the Royal Society of London B: Biological Sciences* **369**(1643):
581 20130194.
582 **McGill BJ, Enquist BJ, Weiher E, Westoby M. 2006.** Rebuilding community ecology from
583 functional traits. *Trends in Ecology & Evolution* **21**(4): 178-185.

584 **McManus KM, Asner GP, Martin RE, Dexter KG, Kress WJ, Field CB. 2016.** Phylogenetic
585 structure of foliar spectral traits in tropical forest canopies. *Remote Sensing* **8**(3): 196.
586 **Meireles JE, Schweiger AK, Cavender-Bares J. 2017.** spectrolab: Class and Methods for
587 Hyperspectral Data. R package version 0.0.2.
588 **Mevik B-H, Wehrens R, Liland KH. 2018.** pls: Partial Least Squares and Principal Component
589 regression. R package version 2.7-0.
590 **Niinemets Ü. 2007.** Photosynthesis and resource distribution through plant canopies. *Plant, cell*
591 *& environment* **30**(9): 1052-1071.
592 **Ollinger SV. 2011.** Sources of variability in canopy reflectance and the convergent properties of
593 plants. *New Phytologist* **189**(2): 375-394.
594 **Palmer MW, Earls PG, Hoagland BW, White PS, Wohlgemuth T. 2002.** Quantitative tools
595 for perfecting species lists. Environmetrics: The official journal of the International
596 Environmetrics Society **13**(2): 121-137.
597 **Petchey OL, Gaston KJ. 2006.** Functional diversity: back to basics and looking forward.
598 *Ecology Letters* **9**(6): 741-758.
599 **Pickett S, Bazzaz F. 1978.** Organization of an assemblage of early successional species on a soil
600 moisture gradient. *Ecology* **59**(6): 1248-1255.
601 **R Core Team 2019**. R: A language and environment for statistical computing. Vienna: R
602 Foundation for Statistical Computing.
603 **Reich PB, Walters MB, Ellsworth DS. 1997.** From tropics to tundra: global convergence in
604 plant functioning. *Proceedings of the National Academy of Sciences* **94**(25): 13730-13734.
605 **Revell LJ. 2012.** phytools: an R package for phylogenetic comparative biology (and other
606 things). *Methods in Ecology and Evolution* **3**(2): 217-223.
607 **Rocchini D, Balkenhol N, Carter GA, Foody GM, Gillespie TW, He KS, Kark S, Levin N,**
608 **Lucas K, Luoto M. 2010.** Remotely sensed spectral heterogeneity as a proxy of species
609 diversity: recent advances and open challenges. *Ecological Informatics* **5**(5): 318-329.
610 **Rozendaal D, Hurtado V, Poorter L. 2006.** Plasticity in leaf traits of 38 tropical tree species in
611 response to light; relationships with light demand and adult stature. *Functional Ecology* **20**(2):
612 207-216.

Schweiger AK, Cavender-Bares J, Townsend PA, Hobbie SE, Madritch MD, Wang R, Tilman D, Gamon JA. 2018. Plant spectral diversity integrates functional and phylogenetic components of biodiversity and predicts ecosystem function. *Nature Ecology & Evolution*.

Schwinning S, Weiner J. 1998. Mechanisms determining the degree of size asymmetry in competition among plants. *Oecologia* **113**(4): 447-455.

Sievert C, Parmer C, Hocking T, Chamberlain S, Ram K, Corvellec M, Despouy P. 2017. plotly: Create Interactive Web Graphics. R package version 4.7.1. *https://CRAN.R-project.org/package=plotly*.

Silvertown J. 2004. Plant coexistence and the niche. *Trends in Ecology & Evolution* **19**(11): 605-611.

Sims DA, Gamon JA. 2002. Relationships between leaf pigment content and spectral reflectance across a wide range of species, leaf structures and developmental stages. *Remote Sensing of Environment* **81**(2-3): 337-354.

Slaton MR, Raymond Hunt Jr E, Smith WK. 2001. Estimating near-infrared leaf reflectance from leaf structural characteristics. *American journal of botany* **88**(2): 278-284.

Springer K, Wang R, Gamon J. 2017. Parallel seasonal patterns of photosynthesis, fluorescence, and reflectance indices in boreal trees. *Remote Sensing* **9**(7): 691.

Tilman D, Knops J, Wedin D, Reich P, Ritchie M, Siemann E. 1997. The influence of functional diversity and composition on ecosystem processes. *Science* **277**(5330): 1300-1302.

Ustin SL, Gamon JA. 2010. Remote sensing of plant functional types. *New Phytologist* **186**(4): 795-816.

Ustin SL, Roberts DA, Gamon JA, Asner GP, Green RO. 2004. Using imaging spectroscopy to study ecosystem processes and properties. *BioScience* **54**(6): 523-534.

Valladares F, Wright SJ, Lasso E, Kitajima K, Pearcy RW. 2000. Plastic phenotypic response to light of 16 congeneric shrubs from a Panamanian rainforest. *Ecology* **81**(7): 1925-1936.

Venables WN, Ripley BD. 2002. Modern applied statistics with S. New York: Springer.

Violle C, Jiang L. 2009. Towards a trait-based quantification of species niche. *Journal of plant ecology* **2**(2): 87-93.

642 **Wang R, Gamon J, Montgomery R, Townsend P, Zygielbaum A, Bitan K, Tilman D,**
643 **Cavender-Bares J. 2016.** Seasonal Variation in the NDVI–Species Richness Relationship in
644 a Prairie Grassland Experiment (Cedar Creek). *Remote Sensing* **8**(2): 128.
645 **Williams LJ, Paquette A, Cavender-Bares J, Messier C, Reich PB. 2017.** Spatial
646 complementarity in tree crowns explains overyielding in species mixtures. *Nature Ecology &*
647 *Evolution* **1**: 0063.
648 **Wold S, Martens H, Wold H 1983**. The multivariate calibration problem in chemistry solved by
649 the PLS method.In Ruhe A, Kagstrom B. *Matrix pencils, Lecture Notes in Mathematics*:
650 Springer, Heidelberg. 286-293.
651 **Wright IJ, Reich PB, Westoby M, Ackerly DD, Baruch Z, Bongers F, Cavender-Bares J,**
652 **Chapin T, Cornelissen JH, Diemer M. 2004.** The worldwide leaf economics spectrum.
653 *Nature* 428(6985): 821-827.
654

Figures

Fig. 1 The unique niche fraction per species increases with increasing dimensionality of the spectral space **(a)** and functional trait space **(b).** Curves represent second order polynomials fitted to 50 estimates of species niche sizes calculated with increasing number of dimensions (2-21 spectral bands and 2-10 functional traits, respectively); 95% confidence interval are shown in grey. The species are *Sorghastrum nutans* (L.) Nash (27 ind., SORNU), *Schizachyrium scoparium* (Michx.) Nash (76 ind., SCHSC), *Andropogon gerardii* Vitman (162 ind., ANDGE), *Panicum virgatum* L. (49 ind., PANVI), *Lespedeza capitata* Michx. (99 ind., LESCA), *Petalostemum villosum* Nutt. (42 ind., PETVI), *Petalostemum purpureum* (Vent.) Rydb. (52 ind., PETPU), *Petalostemum candidum* (Willd.) Michx. (28 ind., PETCA), *Amorpha canescens* Pursh (28 ind., AMOCA), *Lupinus perennis* L. (121 ind., LUPPE), *Solidago rigida* L. (50 ind., SOLRI), *Liatris aspera* Michx. (49 ind., LIAAS), *Achillea millefolium* L. (49 ind., ACHMI), *Asclepias tuberosa* L. (70 ind., ASCTU). The phylogenetic relationships among species are displayed on the right; graminoids are coded in blue, legumes in purple-red-orange and forbs in yellow-grey-black colors.

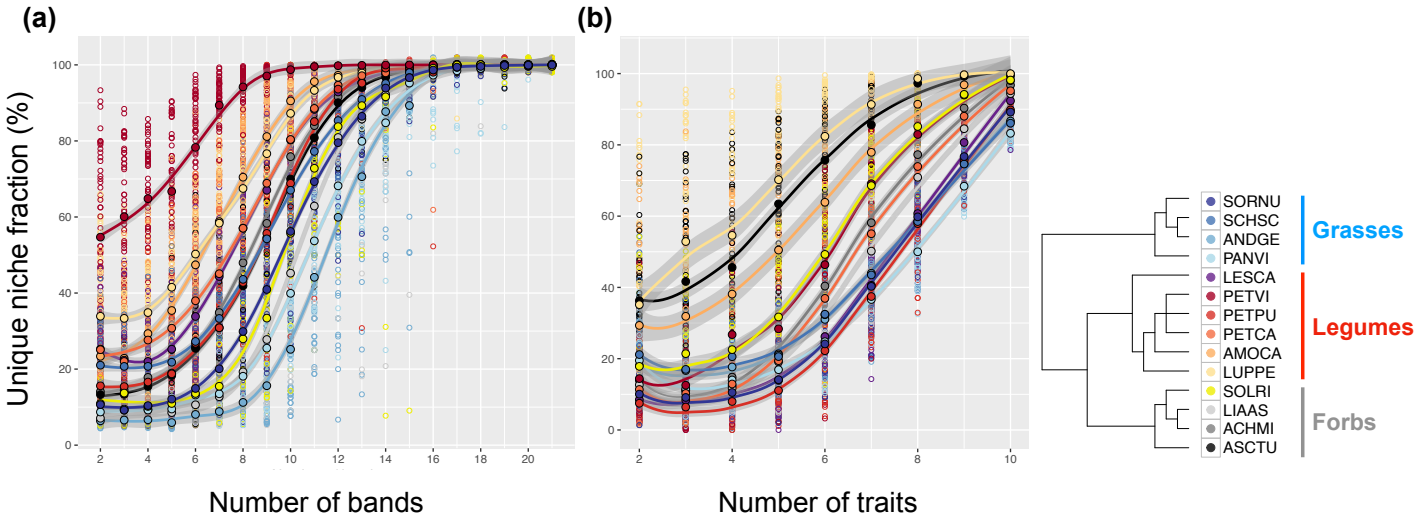

Fig. 2 Species clustering along linear discriminant (LD) axes maximizing the differences among species based on spectra **(a-c)** and functional traits **(d-f)**. The amount of the total variation explained by each LD axis is shown in parentheses; for species abbreviations and number of individuals per species see Fig. 1.

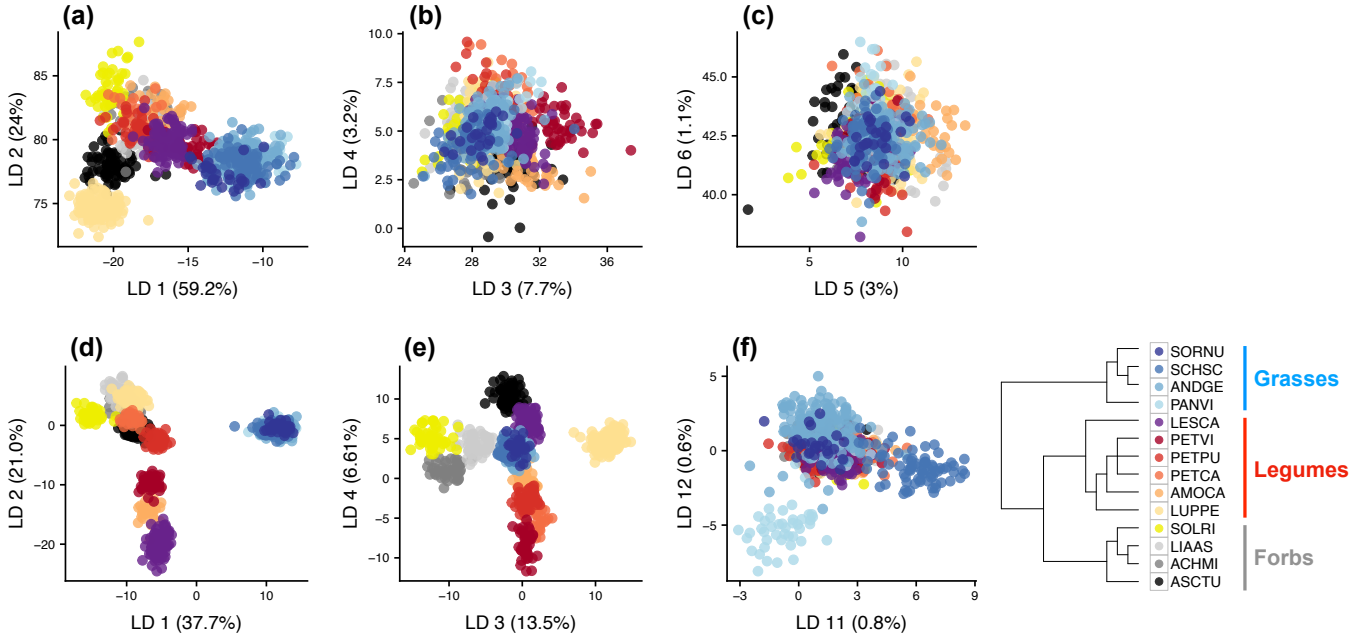

Fig. 3 Probabilities for each species to be classified correctly, or incorrectly classified as another species based on partial least squares discriminant analysis (PLSDA) models using species spectra **(a)** and functional traits **(b)** sampled in the BioDIV experiment in July. PLSDA assigns to every sample the classification probabilities to belong to each class (i.e. species). Colored bars that match the species color, shown at the tip of the phylogeny, indicate the averaged probability that the species was correctly classified. Bars that show a different color indicate the averaged probability that the species was misclassified as a different species. The percentages of correctly classified samples per species in PLSDA are shown in parentheses. For species abbreviations and number of individuals per species see Fig. 1; the graph shows model validation results, i.e. n = the number of individual per species - 20 individuals for model calibration.

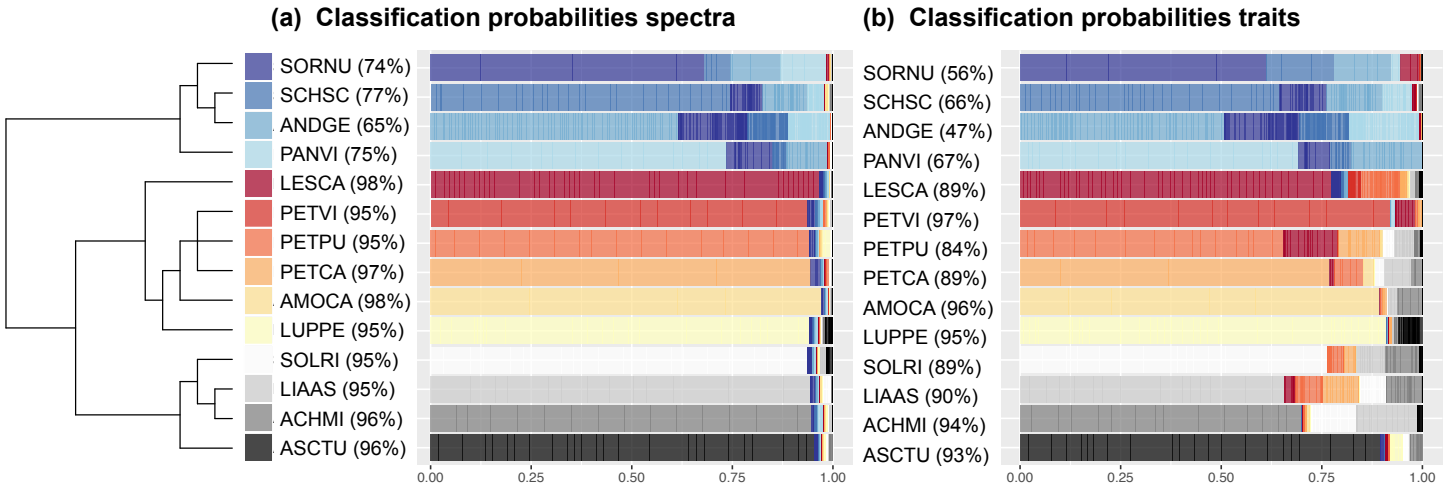

Fig. 4 The spectral space occupied by individual trees in the FAB experiment predicting tree growth. Tree height [**(a)**, n = 532, $R^2 = 0.11$, $F_{1,530} = 63.2$, $P < 0.001$; **(b)**, n = 524, $R^2 = 0.14$, $F_{1,522} = 81.6$, $P < 0.001$], and stem diameter [**(c)**; n = 532, $R^2 = 0.20$, $F_{1,530} = 135.5$, $P < 0.001$; **(d)**, n = 396, $R^2 = 0.25$, $F_{1,394} = 130.2$, $P < 0.001$] were measured in 2016 and 2017, respectively; spectral space sizes are log-transformed; the number of species per plot is indicated with different symbols.

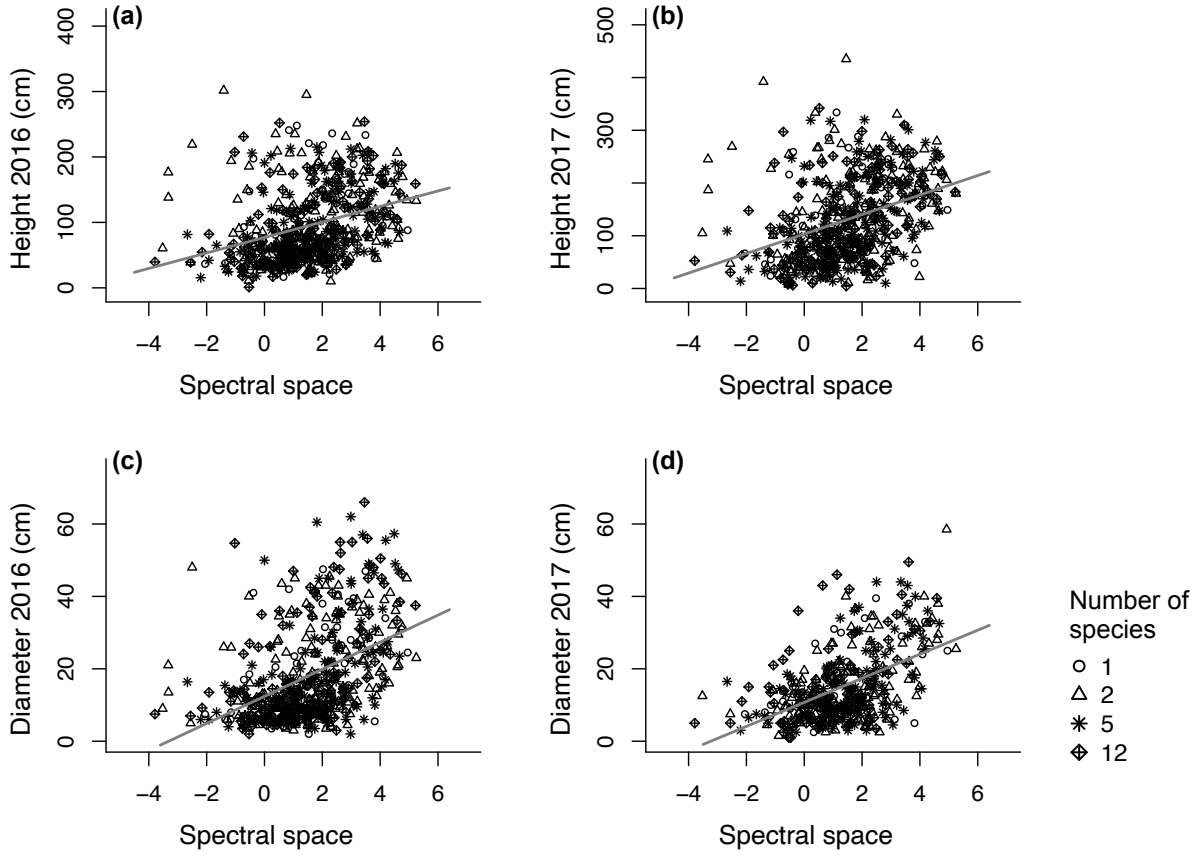

Fig. 5 The spectral space occupied by plant communities predicting aboveground productivity and species richness in the BioDIV experiment. The size of the spectral space occupied per community is calculated from contact measurements of leaf spectra in July [**(a)**, n = 30, R^2 = 0.44, $F_{1,28}$ = 22.6, P < 0.001; **(c)**, n = 30, R^2 = 0.25, $F_{1,28}$ = 9.1, P < 0.001] and from imaging spectroscopy data [**(b)**, n = 18, R^2 = 0.31, $F_{1,16}$ = 7.1, P < 0.017]; species richness (indicated with different symbols) is the number of species planted per plot; aboveground productivity (g m^{-2}) was determined in clip strips the same month; spectral space sizes are log-transformed.

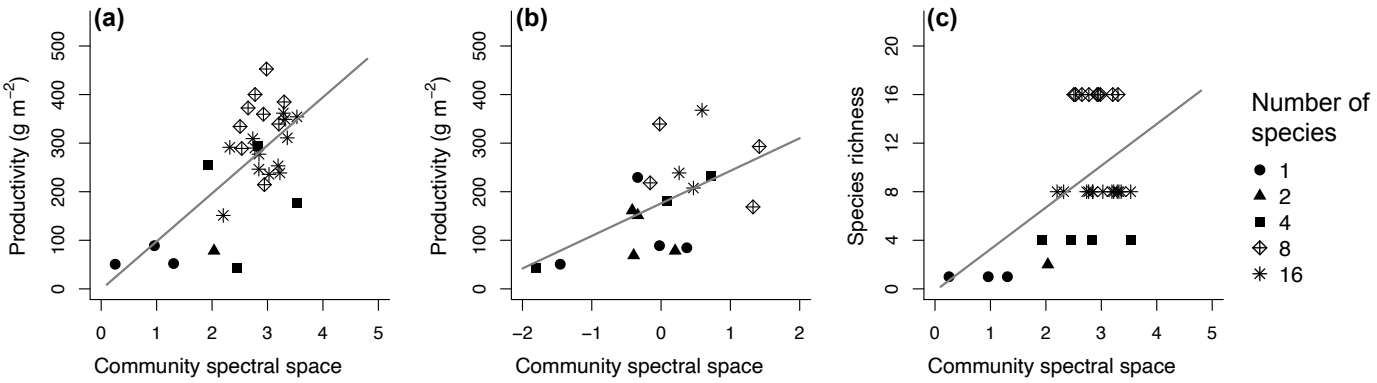

Fig. 6 The spectral space occupied by plant communities predicting the net biodiversity effect [NBE, **(a)**, n = 43, $R^2 = 0.37$, $F_{1,41} = 24.3$, $P < 0.001$] and its two components complementarity [CE, **(c)**, n = 43, $R^2 = 0.36$, $F_{1,41} = 23.4$, $P < 0.001$], and selection effect [SE, **(d)**, n = 43, $R^2 = 0.20$, $F_{1,41} = 10.3$, $P < 0.003$], and species richness [**(b)**, n = 43, $R^2 = 0.20$, $F_{1,41} = 10.5$, $P < 0.003$] in the FAB experiment. The size of the spectral space occupied per community is calculated from contact measurements of leaf spectra; species richness (indicated with different symbols) is the number of species planted per plot; NBE, SE and CE are square root-transformed with signs retained (see Grossman *et al.*, 2017); spectral space sizes are log-transformed.